

RADIOGRAPHIC EVALUATION OF PATHOLOGICAL BONE LESIONS: CURRENT SPECTRUM OF DISEASE AND APPROACH TO DIAGNOSIS

BY BENJAMIN G. DOMB, MD, WAKENDA TYLER, MD, MPH,
SCOTT ELLIS, MD, AND EDWARD MCCARTHY, MD

Introduction

Radiographic evaluation is an extremely powerful tool that allows the orthopaedic surgeon to characterize and classify bone lesions by their appearance and by the reaction of the surrounding bone and soft tissue. Careful and analytical characterization of bone lesions on plain radiographs often enables the surgeon to greatly narrow the differential diagnosis. The goal of this exhibit is to provide the reader with a fundamental algorithm for the radiographic

evaluation of benign and malignant bone lesions. The algorithm is summarized in the flow charts in Figures 1 and 2, which provide a step-by-step process for the classification of lesions. Also shown in the charts are important examples of each category.

Comparison of Radiodense and Radiolytic Lesions

The first step in this approach is to determine whether the lesion is radiodense or radiolytic. At the cellular level, radi-

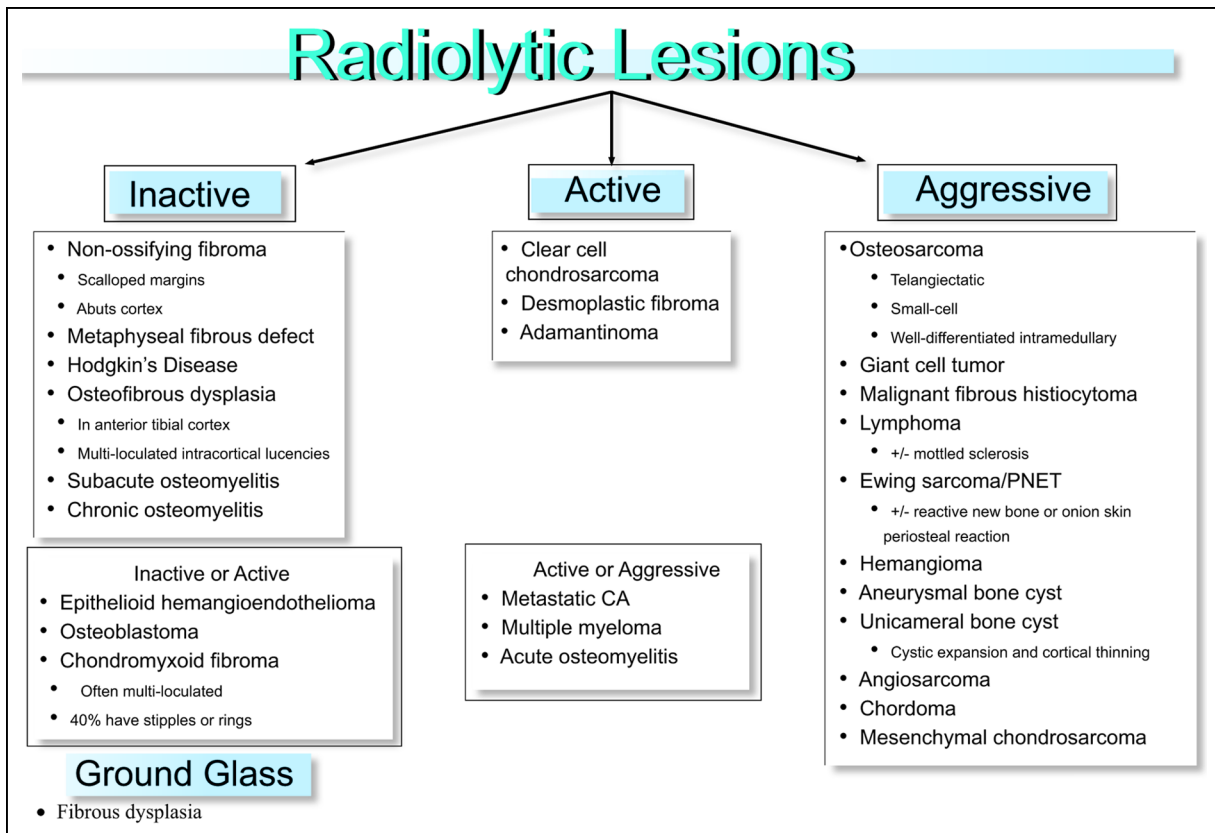


Fig. 1

Algorithm for the classification of radiolytic bone lesions. CA = carcinoma, and PNET = primitive neuroectodermal tumor.

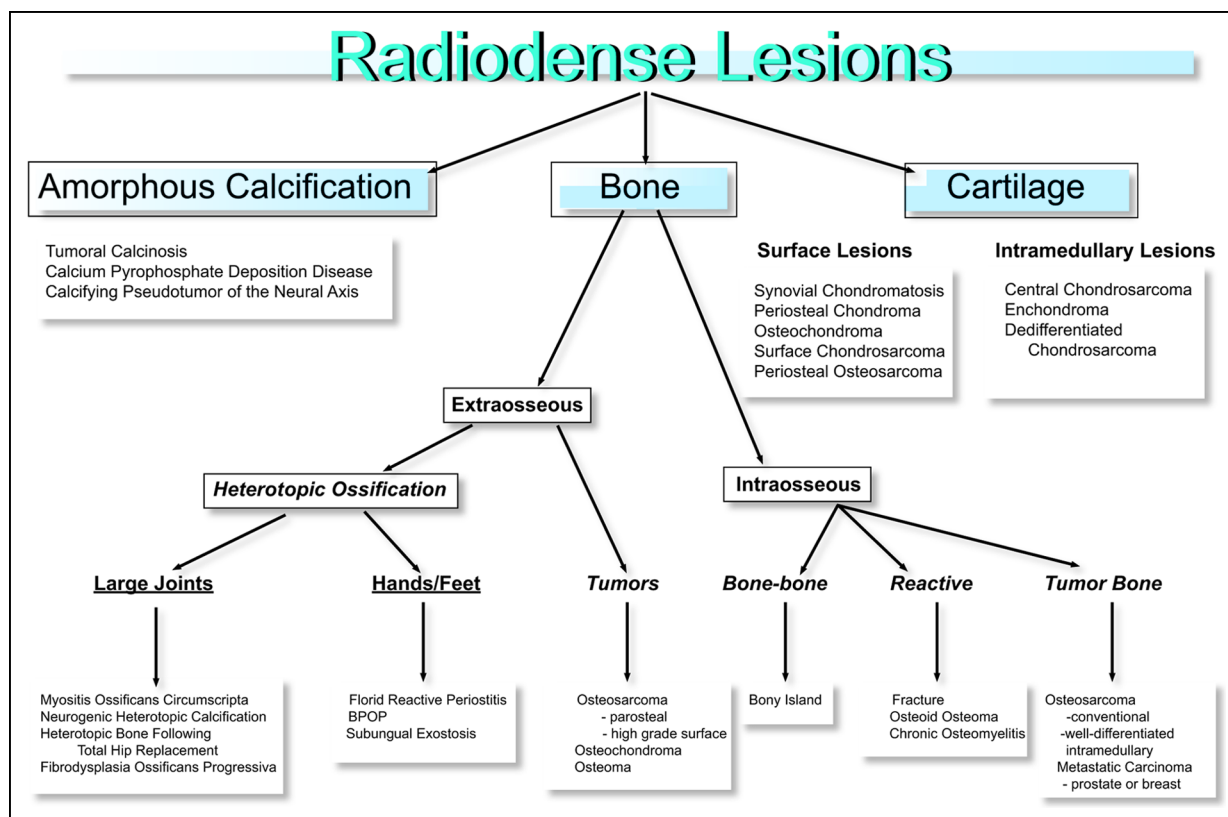


Fig. 2

Algorithm for the classification of radiodense bone lesions. BPOP = bizarre parosteal osteochondromatous proliferation of bone.

olytic lesions have varying degrees of bone reabsorption, which is detected as a lack of calcium on plain radiographs. Radiodense lesions at the cellular level, however, have an overabundance of calcium compared with normal bone, producing their appearance on plain radiographs. This overabundance of calcium may take the form of bone, amorphous calcification, or cartilage¹⁻³.

Radiolytic Lesions

Radiolytic lesions can be broadly classified into four categories on the basis of their radiographic characteristics: inactive, active, aggressive, and ground glass. Inactive lesions are well circumscribed and surrounded by a sclerotic rim of bone. Figure 3 shows an example of an inactive radiolytic lesion—in this case, subacute osteomyelitis of the proximal aspect of the tibia. The lesion has central bone reabsorption, which appears lytic on the radiograph; however, note the sclerotic rim of bone surrounding the lesion. It is clear from this radiograph that the lesion is not growing, and, in fact, the body has had time to create a wall of new reactive bone around the lesion to further contain it.

Figure 4 shows an example of an active lytic lesion of the proximal aspect of the tibia. This giant-cell tumor of the proximal part of the tibia clearly exemplifies the typical characteristics of an active lytic lesion. The lesion is still very well circumscribed with a clear border delineating its margins within the bone. However, unlike the inactive lesion in Figure

3, this lesion has no sclerotic rim. The lack of a sclerotic rim indicates that the lesion is still growing and continuing to reabsorb bone at its borders, not giving the surrounding bone a chance to wall it off.

Figure 5 shows an example of an aggressive lytic lesion of the proximal part of the humerus. In this case, the metastatic tumor shows a permeative process with no clear delineation of its borders. There is also cortical expansion and destruction. This lesion is growing fast and out of control. The body and surrounding bone has no way of defending itself from this aggressive, uncontrolled growth. This is typical of highly malignant bone lesions (such as Ewing sarcoma), acute osteomyelitis, leukemia, and several primary malignant sarcomas of the bone.

Finally, the classic hazy “ground-glass” appearance of fibrous dysplasia is placed in its own category. As shown in Figure 6, fibrous dysplasia is typically a long lesion in a long bone, with thinning of the cortices and occasionally cortical destruction. However, it is distinguished from aggressive lesions by its clearly demarcated borders.

Figure 1 is a flow chart that provides a schematic representation of the way the orthopaedist should go about characterizing and classifying lytic lesions.

Radiodense Lesions

Radiodense lesions can be broadly classified into three categories on the basis of the structure of the material making up the

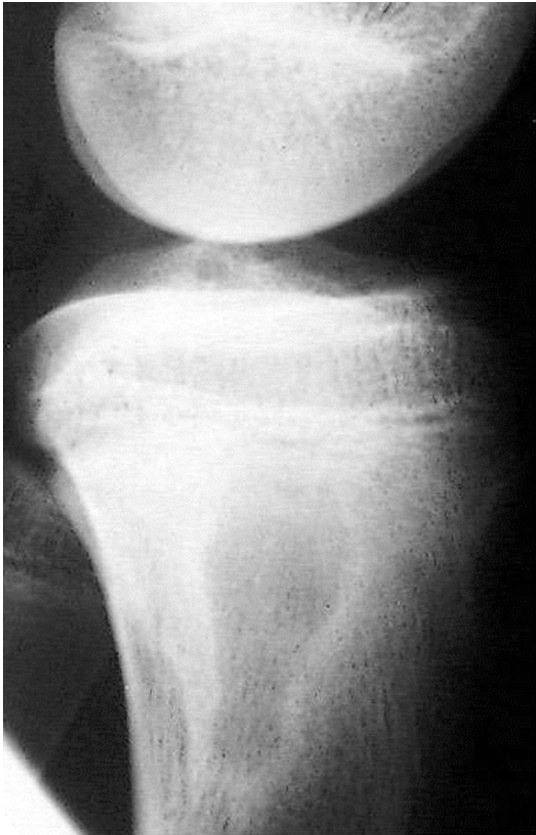


Fig. 3
An inactive radiolytic lesion. This is an example of sub-acute osteomyelitis of the proximal part of the tibia. Note the well-circumscribed sclerotic rim.



Fig. 4
An active lytic lesion. This is an example of a giant-cell tumor of the proximal part of the tibia. Note the absence of a sclerotic rim, but the lesion still has a well-circumscribed nature.

Fig. 5
An aggressive lytic lesion. This is an example of metastatic carcinoma of the proximal aspect of the humerus. Note the cortical expansion and destruction.

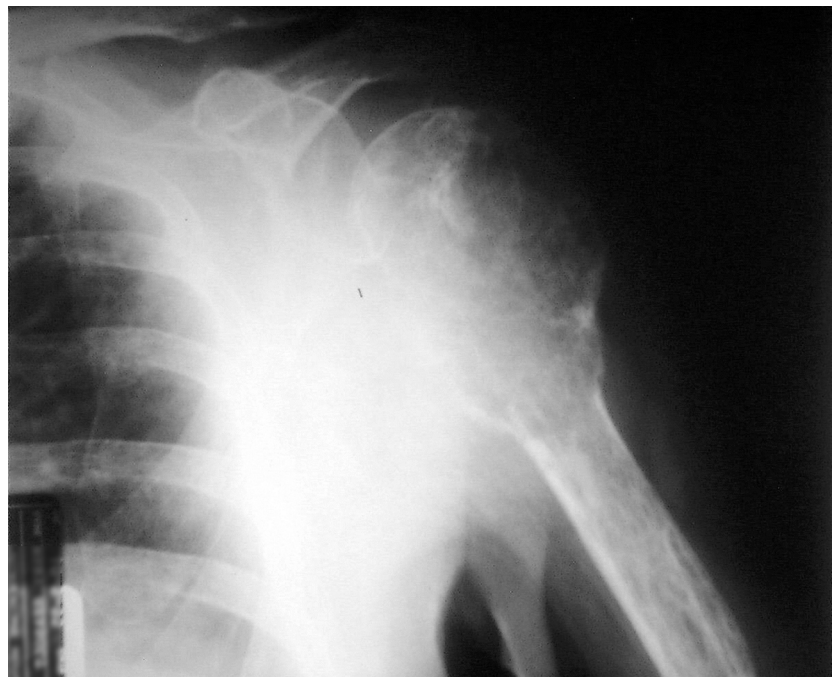




Fig. 6
Fibrous dysplasia of the tibia. Note the ground-glass appearance of this long lesion in a long bone.



Fig. 7
An amorphous calcification of the proximal tibial area. This example of tumoral calcinosis has the classic so-called wet cotton-ball appearance.

lesion. These lesions can be amorphous calcification, bone, or cartilage. Amorphous calcification, as its name implies, is a collection of calcifications without a well-defined matrix. It typically appears on the radiograph as fluffy “wet cotton-ball” calcifications in the soft tissue and bone (Fig. 7)⁴⁵. At the histologic level, bland calcium crystals without a matrix are seen.

Cartilage lesions appear with characteristic rings and stipples on plain radiographs. These rings and stipples correlate histologically to the endochondral ossification at the core and periphery of the cartilage lobules. Both benign and malignant cartilage processes have this radiographic pattern. Cartilaginous lesions may be divided into intramedullary lesions and surface lesions. As in most processes, benign lesions appear well circumscribed while malignant lesions are ill defined. Figure 8 is an example of an enchondroma of the distal aspect of the femur. An enchondroma is an example of a benign intramedullary cartilage lesion. Note the clear rings and stipples present in the medullary canal. Figure 9 is an example of an osteochondroma, a benign extraosseous cartilage bone lesion. Again note the rings and stipples and the well-demarcated nature of this osteochondroma. Also note that the marrow of



Fig. 8
Enchondroma of the distal aspect of the femur. This is a well-circumscribed intramedullary lesion with rings and stipples.



Fig. 9
Osteochondroma of the proximal part of the tibia. This lesion is a benign extraosseous cartilage bone tumor. Note the well-defined margins and its continuity with the medullary canal.



Fig. 10
Heterotopic ossification abutting bone. Note its well-circumscribed nature with a trabecular pattern.

this lesion is continuous with the medullary canal of the proximal aspect of the tibia from which it arises.

All radiodense lesions in the form of bone are characterized by the presence of a matrix at the histologic level, which on plain radiographs appears as a trabecular pattern. Lesions composed of bone may be intraosseous or extraosseous. Extraosseous bone lesions may be divided into heterotopic ossification (well circumscribed) or tumor bone (ill defined). In Figure 10, note the well-circumscribed borders and trabecular pattern that are characteristic of heterotopic ossification. The parosteal osteosarcoma seen in Figure 11 is an example of a malignant extraosseous bone lesion, demonstrating the poorly demarcated border that is typical of such a malignancy.

Intraosseous bone lesions start in the medullary canal, but they also may break through the cortex and extend into the surrounding soft tissue. These lesions can be divided into three categories: normal bone, reactive bone, and tumor bone, each with a distinct radiographic pattern. A bone island (enostosis) is an example of dense normal bone that develops in the medullary canal as a result of a remodeling error that occurs during skeletal growth (Fig. 12). Its appearance in every way looks like normal “misplaced” bone. It has a trabecular pattern that is easily seen on radiographs and is always well circumscribed.



Fig. 11
Parosteal osteosarcoma. This is a poorly circumscribed and patternless extraosseous bone lesion.



Fig. 12
A bone island in the proximal aspect of the humerus. This is a well-circumscribed intraosseous lesion of mature bone.

Reactive bone is characterized by a zonal pattern of bone formation, with smooth transitions from dense areas to normal bone areas. Figure 13 is an example of reactive bone. As the name implies, reactive bone is usually reacting to a process such as infection, fracture, or osteoid osteoma.

Unlike reactive bone and normal bone, tumor bone is characterized by its lack of a pattern. It usually has no clear distinct margins and may present as a combination of lytic and dense blastic areas on plain radiographs. Tumor bone is also noted for its cortical destruction and expansile nature. Figure 14 is a classic example of conventional osteosarcoma of



Fig. 14
A conventional osteosarcoma of the distal aspect of the femur. There is a patternless formation of bone in the medullary canal.

the distal aspect of the femur. Note the patternless density and cortical destruction seen on this radiograph. This same image could also be an example of metastatic carcinoma, another form of tumor bone.

The flow chart in Figure 2 provides an outline of the approach to radiodense lesions of the bone.



Fig. 13
A reactive intraosseous bone lesion. This is an example of an osteoid osteoma. Note the zonal pattern of bone formation.

Conclusions

With the above information, one should now be aware of the radiographic characteristics of the most common pathological bone lesions and should be able to recognize these lesions on plain radiographs using an algorithmic approach to radiographic diagnosis as outlined in Figures 1 and 2. It should be emphasized that this approach is based solely on the plain radiographic appearance and is intended to aid the surgeon in developing an initial differential diagnosis when a lesion is first noted on radiographs. It must be emphasized that the practitioner must combine this approach with an understanding of the common locations of specific lesions, patient characteristics, other imaging modalities, and biopsy results in order to arrive at a correct diagnosis. ■

Corresponding author:

Benjamin G. Domb, MD

Department of Orthopaedics, Hospital for Special Surgery, Office of Academic Training, 535 East 70th Street, New York, NY 10021. E-mail address: bendomb@yahoo.com

The authors did not receive grants or outside funding in support of their research or preparation of this manuscript. They did not receive payments or other benefits or a commitment or agreement to provide such benefits from a commercial entity. No commercial entity paid or directed, or agreed to pay or direct, any benefits to any research fund, foundation, educational institution, or other charitable or nonprofit organization with which the authors are affiliated or associated.

References

1. **Sweet DE, Madewell JE, Ragsdale BD.** Radiologic and pathologic analysis of solitary bone lesions. Part III: matrix patterns. *Radiol Clin North Am.* 1981;19:785-814.
2. **Ragsdale BD, Madewell JE, Sweet DE.** Radiologic and pathologic analysis of solitary bone lesions. Part II: periosteal reactions. *Radiol Clin North Am.* 1981;19:749-83.
3. **Madewell JE, Ragsdale BD, Sweet DE.** Radiologic and pathologic analysis of solitary bone lesions. Part I: internal margins. *Radiol Clin North Am.* 1981; 19:715-48.
4. **McCarthy EF, Frassica FJ.** *Pathology of bone and joint disorders: with clinical and radiographic correlation.* Philadelphia: Saunders; 1998.
5. **Steinbach LS, Johnston JO, Tepper EF, Honda GD, Martel W.** Tumoral calcinosis: radiologic-pathologic correlation. *Skeletal Radiol.* 1995;24: 573-8.